

Decreased accumulation of ultrasound contrast in the liver of nonalcoholic steatohepatitis rat model

Yuki Miyata, Takeo Miyahara, Fuminori Moriyasu

Yuki Miyata, Takeo Miyahara, Fuminori Moriyasu, Department of Gastroenterology and Hepatology, Tokyo Medical University, 6-7-1, Nishi-Shinjuku, Shinjuku-ku, Tokyo 160-0023, Japan

Author contributions: Miyata Y and Miyahara T contributed equally to this work; Moriyasu F designed research; Miyata Y and Miyahara T performed research; Miyata Y and Miyahara T contributed new reagents/analytical tools; Miyata Y wrote the paper.

Correspondence to: Fuminori Moriyasu, MD, Department of Gastroenterology and Hepatology, Tokyo Medical University, 6-7-1, Nishi-Shinjuku, Shinjuku-ku, Tokyo 160-0023, Japan. moriyasu@tokyo-med.ac.jp

Telephone: +81-3-53256838 Fax: +81-3-53256840

Received: February 11, 2011 Revised: April 7, 2011

Accepted: April 14, 2011

Published online: October 7, 2011

of contrast ultrasonography may be valuable for non-invasive diagnosis of NASH.

© 2011 Baishideng. All rights reserved.

Key words: Nonalcoholic steatohepatitis; Leptin; Kupffer cell; Methionine choline-deficient diet; Contrast ultrasound

Peer reviewer: Søren Rafaelsen, MD, Consultant Radiologist, Associate Professor, Department of Radiology, Vejle Hospital, Vejle 7100, Denmark

Miyata Y, Miyahara T, Moriyasu F. Decreased accumulation of ultrasound contrast in the liver of nonalcoholic steatohepatitis rat model. *World J Gastroenterol* 2011; 17(37): 4191-4198 Available from: URL: <http://www.wjgnet.com/1007-9327/full/v17/i37/4191.htm> DOI: <http://dx.doi.org/10.3748/wjg.v17.i37.4191>

Abstract

AIM: To investigate the diagnosis of nonalcoholic steatohepatitis (NASH) using contrast ultrasonography in the NASH rat model.

METHODS: The liver in methionine choline-deficient diet (MCDD) rats, a NASH model constructed by feeding an MCDD, was examined by contrast ultrasonography at weeks 2, 4, 8, 12 and 16, with late phase images of contrast ultrasonography (Kupffer imaging) in which contrast enhancement was achieved by incorporation of a contrast agent by Kupffer cells (KCs), and images were compared to those in rats taking a regular chow.

RESULTS: Decrease in contrast enhancement was observed first in MCDD rats at week 2. KCs were counted based on immunohistochemistry, but their numbers were not reduced and it was assumed that attenuation of contrast enhancement was attributable to reduced phagocytic activity of the KCs.

CONCLUSION: It is suggested that clinical application

INTRODUCTION

Nonalcoholic steatohepatitis (NASH) is a relatively new disease entity, proposed by Ludwig in 1980^[1], which exhibits a clinical manifestation similar to that of alcoholic steatohepatitis in terms of liver histology, despite a lack of history of alcohol abuse causing hepatitis. The diagnosis of fatty liver without a history of drinking alcohol is generally termed nonalcoholic fatty liver disease (NAFLD), which is most simply fatty liver with an excellent prognosis, while NASH is a subtype of NAFLD^[2].

It is important to differentiate NASH from NAFLD at an early stage to start relevant treatment. Although there have been a number of reports aimed at differentiating NASH patients^[2], histological diagnosis based on liver biopsy is the only diagnostic method at present. However, liver biopsy is an invasive method, with a small risk of complications, and is too invasive for diagnosis of a benign disease, such as NASH.

It has been previously reported that liver-specific

Kupffer images of contrast ultrasound can be used for differential diagnosis between NASH and NAFLD^[3]. In this study, using a rat model of NASH, we carried out contrast ultrasonography to compare contrast enhancement between the NASH model and control rats that were fed a regular chow. LevovistTM (Schering AG, Berlin, Germany) and SonazoidTM (GE Healthcare, Oslo, Norway) were used as contrast ultrasonography agents. Microbubbles of LevovistTM and SonazoidTM are phagocytosed and incorporated by Kupffer cells (KCs) in the late contrast phase (Kupffer imaging)^[4]. There is a report that contrast enhancement by the contrast agent in the late contrast phase was decreased in patients diagnosed with NASH, compared to NAFLD patients^[3,5]. The reason for decreased microbubble accumulation in the NASH liver is presumed to be because phagocytosis of microbubbles by KCs is decreased.

We constructed a NASH model by feeding a methionine choline-deficient diet (MCDD, Oriental Yeast Co., Tokyo, Japan) to rats^[6-8]. Then, examining the liver using contrast ultrasonography, we compared the phagocytic activity by KCs in rats eating an MCDD and those given regular chow, using contrast enhancement in the late contrast phase.

MATERIALS AND METHODS

Animals and construction of a NASH model

Male Wistar rats weighing about 50 g at the time of purchase were used and kept in a room at 21 °C ± 2 °C with a 12-h cycle of light and darkness. The NASH model was constructed by feeding an MCDD to 15 rats, and the group was designated the MCDD group. Conversely, a diet of regular chow was fed to 5 rats and they were designated the control group. Rats were subjected to experiments at 2, 4, 8, 12 and 16 wk after beginning the diet, and three rats in the MCDD group and one in the control group were used for experiments at each time point. During the follow-up period, water and regular chow were given *ad libitum*. Body weight was measured in all rats in both groups at the designated time points. In addition, to observe the histological changes in liver tissue in MCDD rats at the designated time points, part of the resected liver was fixed in 10% formalin after the experiments, and paraffin slices were prepared and stained with hematoxylin and eosin for histological examination. All animals received humane care and the experimental protocols were approved by the Animal Ethical Committee of Tokyo Medical University.

Incorporation of the contrast ultrasonography agent

After rats were anesthetized at the designated time point by inhalation of diethyl ether (Wako Pure Chemical Industries, LTD., Tokyo, Japan), the abdomen and thighs were shaved and the fascia exposed by an excision of abdominal skin. At the same time, the thigh was incised to expose the femoral vein and a 24-gauge indwelling needle (TERUMO Corp., Tokyo, Japan) was inserted to secure

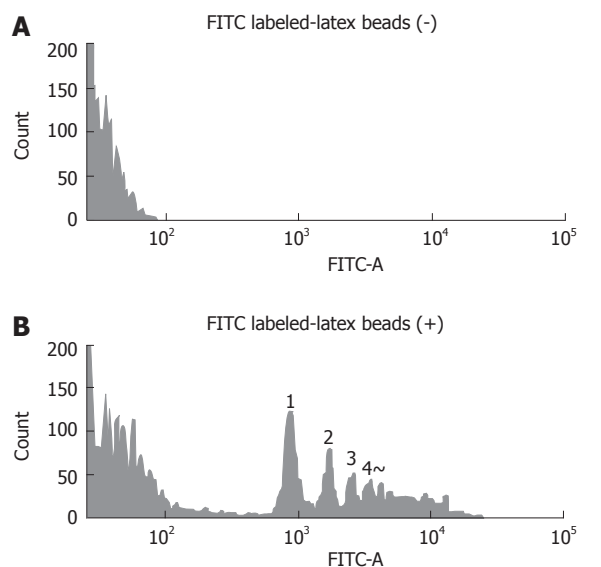
the vessel. From this site, a total of 500 µL of LevovistTM solution (10 µL/g body weight) with physiological saline was infused as a bolus. In both groups, the liver was scanned through the exposed fascia with an echo probe 10 min later. Images were scanned at mechanical index (MI) of 1.5 and then any LevovistTM remaining in the liver was destroyed by sweep scanning over the whole liver. Next, as for LevovistTM, a total of 500 µL of SonazoidTM 10 times diluted solution (1 µL/g of SonazoidTM solution/body weight) with physiological saline was infused intravenously as a bolus and, 10 min later, images were scanned and recorded at Advanced Dynamic FlowTM (ADF) ultrasound mode at MI of 1.5. An AplioTM (Toshiba Medical Systems, Tokyo, Japan) was used in this study. The frequency used was 7.5 MHz and the type of the transducer was linear. ADF was harmonic power Doppler mode from Toshiba Medical Systems.

A region of interest (ROI) was determined arbitrarily in the constant area of ultrasound images of the liver parenchyma obtained at 10 min, and contrast enhancement was quantified in the MCDD and control groups by intensity analysis software Image J (<http://rsb.info.nih.gov/ij/>). Quantified values in the MCDD group were expressed as relative values compared to those in the control group at each designated time point. An ROI was set in the region covering a wide area of the liver parenchyma, excluding large vessels as far as possible. The average intensity in the ROI was measured and relative values were compared.

In vivo administration of FITC-latex beads and isolation of KCs

After experiments using contrast ultrasound, 50 µL of FITC-latex beads (2 µm in diameter, Polyscience, Warrington, PA, United States) were mixed with 500 µL of physiological saline and infused from the tail vein to examine the phagocytic activity of KCs in rats in the MCDD and control groups. One hour later, KCs were isolated according to the following methods: Rats were anesthetized by inhalation of diethyl ether and a midline abdominal incision was made. A 20-G indwelling needle was inserted into the portal vein and after perfusion with Hanks Balanced Salt Solution (HBSS, Sigma, St. Louis, MO, United States), the portal vein was perfused with 100 mL of Dulbecco's Modified Eagle's Medium (DMEM/F-12, Sigma) containing 200 mg pronase (Roche Diagnostics Corp., Indianapolis, IN, United States), followed by 100 mL of DMEM/F-12 containing 25 mg collagenase (Nitta Gelatin Inc., Osaka, Japan). When collagenase leaked out of the blood vessel because of rupture during perfusion, and it was judged that the liver was not perfused, the procedure was stopped. After completion of perfusion, the digested liver was extracted carefully and incubated in DMEM/F-12 supplemented with 0.035% pronase and 62.5 units/mL of DNase (Sigma) for 20 min at 37 °C on a shaker incubator.

Next, the suspension was filtered through gauze and undigested liver tissue was discarded. The liver cell sus-



$$\text{KC phagocytic index} = [\text{FITC (+) cells} / \text{total KC (gated cells)}] \times 100\%$$

Figure 1 Measurement of Kupffer cells phagocytic activity by flow cytometry. A: The negative control, into which fluorescein isothiocyanate (FITC)-labeled latex beads were not injected; B: The positive control to which FITC-labeled latex beads were administered. Note the several peaks of the FITC from the beads in the positive control. The numbers on the peak shows the number of latex beads phagocytosed. KC: Kupffer cell.

pension containing KCs was centrifuged for 1 min at 50 *g*/min and the supernatant collected. Then, the supernatant was centrifuged again at 50 *g*/min and parenchymal liver cells were removed as far as possible. Subsequently, the supernatant was centrifuged at 500 *g*/min for 8 min and a pellet of non-parenchymal cells was obtained. The supernatant was discarded and the pellet was resuspended with a small amount of washing buffer. The non-parenchymal liver cell suspension containing KCs was centrifuged at 900 *g*/min for 15 min with 50% and 25% Percoll (Pharmacia, Uppsala, Sweden) for density-gradient centrifugation, and the first layer from the top was collected. Next, the suspension was rinsed with 40 mL of HBSS and percentages of KCs that had phagocytosed FITC-latex beads were measured by flow cytometry. The purity of the KCs was examined by incorporation of latex beads 2 μm in size and confirmed to be always 96% or greater. Viability was examined by the trypan blue dye exclusion test and unstained cells accounted for 90% or more.

Changes in phagocytic activity of KCs

Phagocytosis by KCs isolated from each group was examined using a BD LSR-II flow cytometer (Becton Dickinson, Franklin Lakes, NJ, United States). First, in a preliminary experiment, it was determined whether FITC-latex beads phagocytosed by KCs were measurable by the flow cytometer. The flow cytometry histogram of KCs in the control group is shown in Figure 1. The upper panel shows the flow cytometer histogram of KCs in the control rat without adding FITC-latex beads and

the lower panel shows the flow cytometer histogram of KCs in the control rat given FITC-latex beads. The amount of FITC-latex beads added was the same as in the subsequent experiments. There were peaks representing the number of FITC-latex beads, but the number of KCs that phagocytosed five beads or more was not determined. Nevertheless, it was possible to detect phagocytosed FITC-latex beads. KCs isolated in the control group were used to determine the position of gating and the gates were set a little wider. After the flow of 10 000 counts of KCs, the percentage of cells positive for fluorescence of FITC-latex beads in all gated cells was calculated in the MCDD and control groups and taken as the phagocytic activity.

Changes in KCs

Because there was a possibility that microbubble accumulation in the liver was dependent on the number of KCs in the liver, the liver was removed from one rat in each group, embedded in O.C.T. compound (Sakura Finetechnical Co. LTD, Tokyo, Japan) and snap-frozen immediately in liquid nitrogen. Later, 5 μm frozen sections were cut with a cryostat. Sections were fixed with acetone and subjected to immunohistochemistry for KCs with anti-rat macrophage antibody (ED2, SEROTEC Ltd, Oxford, United Kingdom) to count positive cells under the same magnification in the MCDD and control groups. In addition, 5 μm frozen liver specimens were cut with the cryostat and immunofluorescent latex beads were observed.

Statistical analysis

Unpaired Student's *t* test was employed for all statistical analyses and a *P* value less than 0.01 was considered statistically significant.

RESULTS

Body weight changes and liver histology in the MCDD and control groups

Body weight initially was about 50 g and increased in the MCDD group to 270 g at week 9, but decreased slightly thereafter. Although body weight reduced, general conditions were stable. In the control group, body weight increased steadily to about 440 g at week 16. General conditions also were stable (data not shown). In terms of histological changes in the liver, large-droplet fat deposition was recognized in the entire liver lobules at week 2 and later. At week 8, necrotic inflammatory changes were observed around the central vein and inflammatory findings were evident. At week 16, fibrosis was observed extending from the central vein and the MCDD group was judged to be a NASH model. In contrast, no fatty liver, inflammation, or fibrosis was observed up to week 16 in the control group (Figure 2).

Changes in contrast ultrasonographic findings

Signal intensity of the liver obtained by contrast ultrasound with LevovistTM was compared between the two groups.

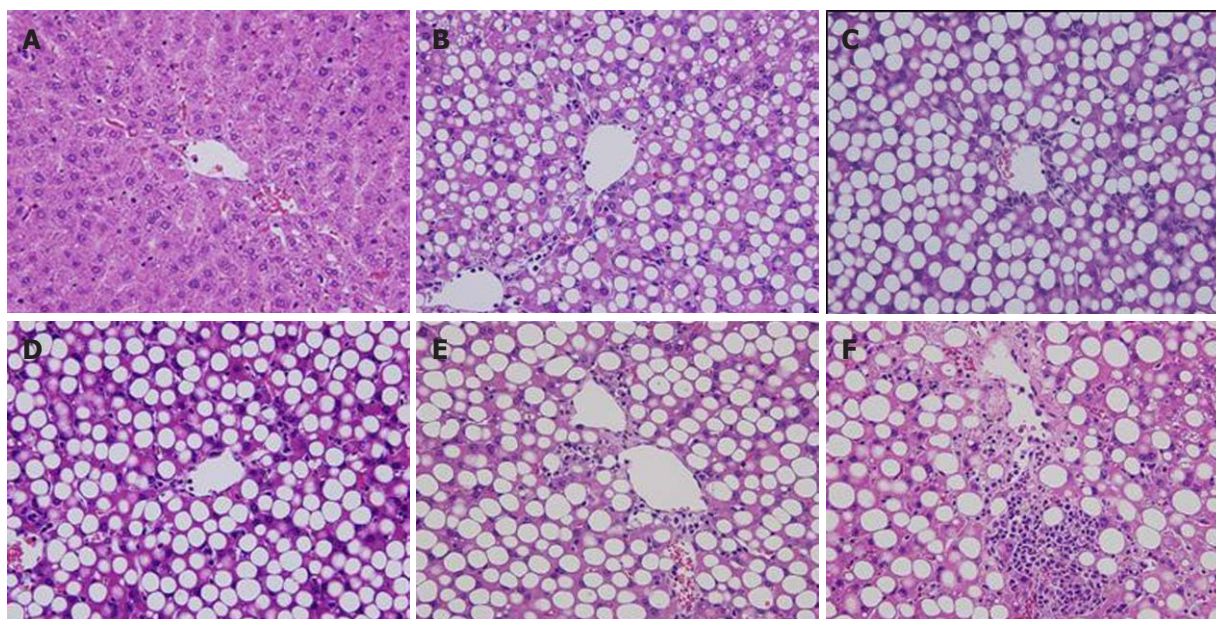


Figure 2 Histological changes of methionine choline-deficient diet-fed rat liver (hematoxylin eosin x 200). Extremely large vesicle fat deposits in almost the entire lobules were detected even as early as two weeks after the start of the methionine choline-deficient diet. By 8 wk, spotty necrosis was dispersed and by 16 wk, there was fibrosis extending from the central vein. A: Control; B: Two weeks methionine choline-deficient (MCD); C: Four weeks MCD; D: Eight weeks MCD; E: Twelve weeks MCD; F: Sixteen weeks MCD.

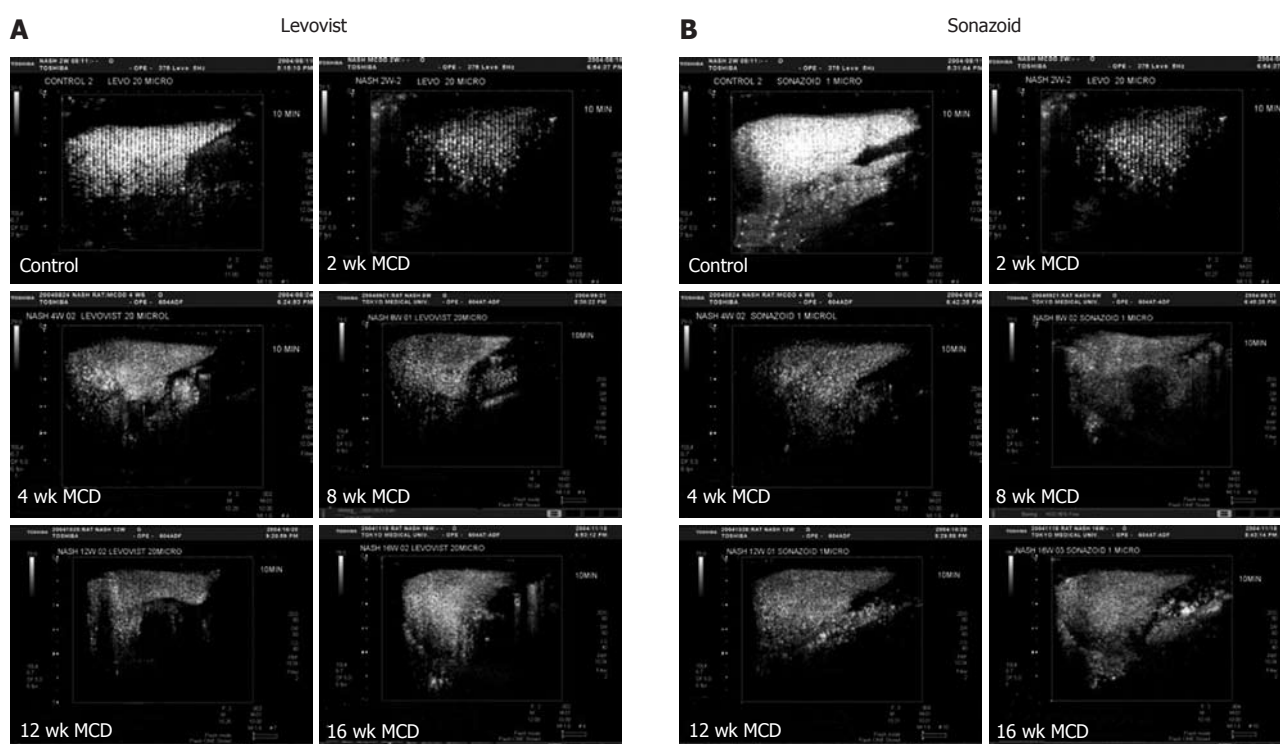


Figure 3 Ultrasound images of the liver 10 min after Levovist™ (A) and Sonazoid™ injection (B). Note signal intensity of the liver was lower in all methionine choline-deficient diet rats than in the controls. MCD: Methionine choline-deficient.

In the MCDD group, the intensity showed a significant decrease at weeks 2, 8 and 12, and a decrease, although not significant, at weeks 4 and 16 (Figures 3A and 4A). On the other hand, signal intensity of the liver obtained by contrast ultrasound with Sonazoid™ showed a significant decrease at all weekly time points in the MCDD group,

compared to the control group (Figures 3B and 4B).

Phagocytic activity of KCs in each group

Phagocytic activities (control *vs* MCDD) of KCs examined with fluorescent latex beads were $44.3\% \pm 12.6\%$ *vs* $18.5\% \pm 9.8\%$ ($P < 0.01$) at week 2, $55.1\% \pm 0.1\%$ *vs*

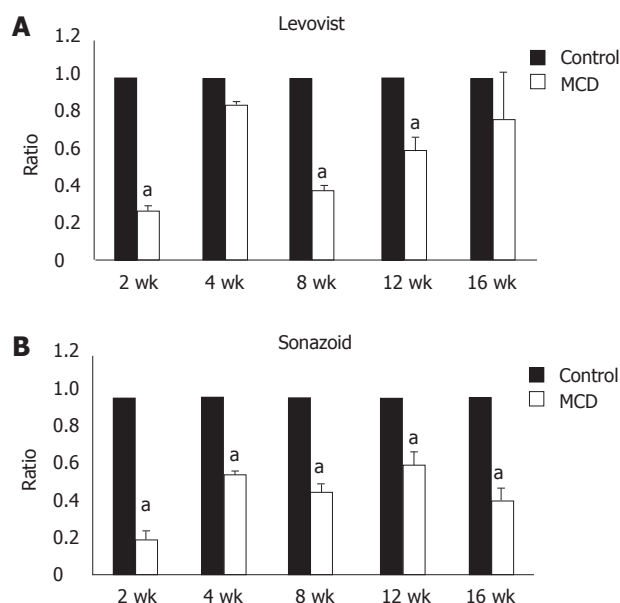


Figure 4 Changes in the signal intensity between control and methionine choline-deficient diet livers. A: Levovist™ contrast enhanced ultrasonography (CEUS). In the methionine choline-deficient diet (MCDD) liver, there was a significant decrease in Levovist™ signal intensity, compared to control livers at 2, 8 and 12 wk. While there was a lower tendency in signal intensity in MCDD liver than control liver at 4 and 16 wk, however, significance was not obtained; B: Sonazoid™ CEUS. In the MCDD liver, there was a significant decrease in Sonazoid™ signal intensity, compared to control livers at all time points. MCD: Methionine choline-deficient. ^a $P < 0.05$ vs control.

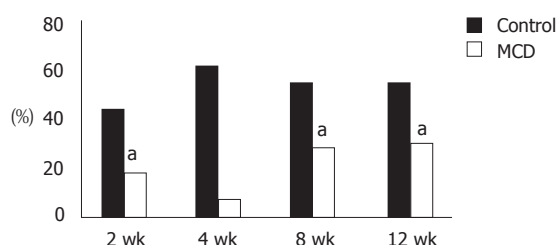


Figure 5 Decreased phagocytic activity in Kupffer cells from methionine choline-deficient diet rats compared to Kupffer cells from control rats. Control and methionine choline-deficient diet (MCDD) rats were injected with fluorescein-isothiocyanate (FITC)-labeled latex beads and Kupffer cells (KCs) were isolated 1 h later. KCs which had phagocytosed FITC-labeled latex beads were counted by flow cytometry and changes in the phagocytic activity were compared between control and MCDD KCs. Note that there was an almost 50% decrease in phagocytic activity in KCs from MCDD, compared to KCs from controls. ^a $P < 0.05$ vs control.

18.5% \pm 9.8% ($P < 0.01$) at week 8, and 57.4% \pm 3.4% *vs* 30.3% \pm 0.6% ($P < 0.01$) at week 12, and the activities in the MCDD group were about half those in the control group. At week 4, only one rat was examined but the activities were 61.9% in the control and 7.6% in the MCDD group, and again they tended to be lower in the MCDD group (Figure 5).

Counting of KCs and images of phagocytosed fluorescent latex beads

Because the decrease in the accumulation of the ultrasound contrast agent in the MCDD group potentially was

Table 1 Numbers of Kupffer cells

Group ($n = 10$)	¹ Total ED-2(+) cells
Control	122 \pm 14
MCDD	² 110 \pm 25

Numbers of Kupffer cells (KCs) in control and methionine choline-deficient diet (MCDD) livers were counted after immunostaining with ED-2 antibody, which recognizes residential macrophages or KCs in the liver. There was no significant difference in the numbers of KCs between controls and MCDD livers. ¹mean \pm SD; ²No significance.

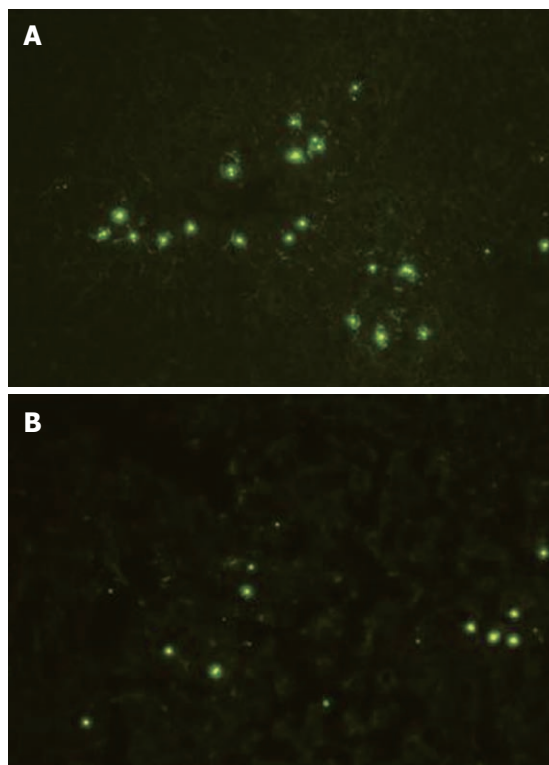


Figure 6 Fluoresceinisothiocyanate-labeled latex beads were injected through the tail veins of control and methionine choline-deficient diet rats. One hour later, small samples of the liver were snap frozen and sectioned using a cryostat. After immediate drying, unfixed tissues were observed by fluorescence microscopy. Note that there were fewer fluoresceinisothiocyanate-labeled latex beads in the livers from methionine choline-deficient diet (B) compared to the controls (A). Magnification: $\times 200$.

attributable to a decrease in the number of KCs compared to the control group, KCs were counted histologically based on immunohistochemistry with anti-rat macrophage antibody. As a result, there was no significant difference between the MCDD and control groups in the number of KCs (Table 1). In addition, fluorescence microscopy revealed a decrease in the accumulation of fluorescent latex beads in the MCDD group compared to the control group (Figure 6).

Serum leptin concentrations

Serum leptin concentrations (control *vs* MCDD) were 120.6 ng/L \pm 39.4 ng/L *vs* 31.5 ng/L \pm 77.6 ng/L ($P < 0.01$) at week 2, 396.7 ng/L \pm 95.0 ng/L *vs* 99.3 ng/L \pm

14.5 ng/L ($P < 0.01$) at week 4, $618.6 \text{ ng/L} \pm 0 \text{ ng/L}$ vs $79.2 \text{ ng/L} \pm 7.0 \text{ ng/L}$ ($P < 0.01$) at week 8, and $397.2 \text{ ng/L} \pm 221.3 \text{ ng/L}$ vs $93.7 \text{ ng/L} \pm 21.5 \text{ ng/L}$ ($P < 0.01$) at week 12, and were significantly lower in the MCDD group at all time points.

DISCUSSION

Fatty liver disease is a state in which triglycerides accumulate in hepatocytes. A manifestation of fat-related liver disease in non-drinkers is known as NAFLD, and consists of simple fatty liver and NASH accompanied by inflammatory changes. At present, it is difficult to differentiate NASH patients from a number of NAFLD patients by any diagnostic method other than liver biopsy. However, biopsy is invasive and potentially causes critical complications. Because it has been reported that 5% of NAFLD patients develop liver cirrhosis^[9], it is important to diagnose NASH at an early stage. There have been reports of differentiating NASH patients from NAFLD patients without the invasiveness of liver biopsy^[2,10]. It has been reported that contrast enhancement is decreased in the late contrast phase in NASH patients compared to healthy subjects^[3,5]. In this study, contrast enhancement was compared by injection of the contrast ultrasonography agent in a NASH model receiving MCDD and in controls taking a regular chow.

MCDD rats have been used in research to investigate the pathogenesis of NASH^[6,11,12]. We used MCDD rats as the most general NASH model developing steatohepatitis, which was induced quickly and easily by the administration of MCDD alone. In this study, the rats started to show fat deposition two weeks after the beginning of MCDD administration, steatohepatitis at week 8 and fibrosis at week 16.

LevovistTM is a first generation ultrasound contrast agent consisting of air as the inner gas within a lipid shell. SonoVueTM, OptisonTM, DefinityTM, ImagentTM and SonazoidTM are available commercially for liver imaging. LevovistTM and SonazoidTM are easily phagocytosed by KCs^[13] and have a liver-specific contrast phase. The ultrasound contrast agent LevovistTM, a high MI contrast agent consisting of microbubbles, is destroyed when exposed to ultrasound with a high acoustic pressure. Most Doppler signals are retrieved when all microbubbles in the scan volume are destroyed with high MI ultrasound. On the other hand, SonazoidTM is a new-generation ultrasound contrast agent, and develops resonance and vibration under the conditions of lower acoustic pressure than that for LevovistTM, because of an elastic phospholipid shell around the inner gas, perfluoro-butane. It is a low MI contrast agent to visualize harmonic signals. Compared to LevovistTM, SonazoidTM has the advantage of enabling evaluation of contrast enhancement in a real-time manner.

In order to quantify the accumulated microbubbles in the liver parenchyma, we destroyed microbubbles by exposing high MI ultrasound to both contrast agents, Levo-

vistTM and SonazoidTM. The period of about 2 min from the injection of the ultrasound contrast agent reflects the early vascular phase, while the time period from about 10 min later reflects the delayed parenchymal phase, or Kupffer imaging, representing the time for phagocytosis of microbubbles by KCs^[14,15]. Therefore, in the delayed parenchymal phase, it is possible to obtain information similar to that provided by superparamagnetic iron oxide (SPIO)-enhanced MRI^[16]. Clinically, about 25% of the ultrasound contrast agent injected from the peripheral vein is phagocytosed by KCs and visualized as the hepatic parenchyma-specific contrast^[17]. It has been reported that dysfunction of KCs is involved in NAFLD^[18].

In this study, images were scanned to measure the signal intensity 10 min after infusion of the ultrasound contrast agent, and accumulation of the medium by KCs was compared between the MCDD and control groups. As a result, contrast enhancement was decreased in MCDD rat livers, as in clinically diagnosed NASH patients. There are two potential mechanisms for the decrease of contrast enhancement in Kupffer imaging, which represents phagocytosis of microbubbles by KCs. These mechanisms are a reduction in phagocytosis by KCs and a decrease in the number of KCs despite normal phagocytic activity. To count the number of KCs, KCs were immunostained with anti-rat macrophage antibody, and it was found that there was no statistical difference in the number of KCs. Therefore, it was thought that decrease of contrast enhancement was attributable to a reduction in phagocytic activity of KCs, rather than a decrease in the number of KCs.

As for the pathogenesis of NASH, phagocytic activity of KCs and involvement of leptin have been suggested. Leptin is an adipocytokine produced by adipose tissue which interacts with a receptor in the hypothalamus. Leptin controls the amount of body fat by suppressing appetite and stimulating sympathetic nerve activity. NAFLD patients with obesity and insulin resistance exhibit leptin resistance and, thereby, serum leptin concentrations increase^[18].

In *ob/ob* mice defective in the leptin gene^[19], fatty liver is present in association with insulin resistance and obesity, and leptin administration improves fatty liver^[20]. In addition, *db/db* mice harboring an abnormality in the leptin receptor do not respond to leptin and develop obesity and fatty liver, as do *ob/ob* mice. Loffreda isolated and cultured macrophages from the peritoneum and bone marrow in *db/db* mice (with abnormality in the leptin receptor) and *ob/ob* mice (deficient in the leptin gene), added *Candida parapsilosis*, and examined the phagocytic activity of macrophages in the groups with and without addition of leptin. Phagocytic activity was augmented in the *ob/ob* mice but unchanged in the *db/db* mice by addition of leptin, which suggested the possibility that leptin interacted directly with KCs to regulate phagocytic activity^[21].

Sakaida *et al*^[22] examined lipopolysaccharide (LPS)-induced phagocytic activity and production of TNF- α in

the KCs isolated from *fa/fa* rats, with a mutation in the leptin receptor gene, and reported that both were reduced compared to the control (*fa/-* rats) and therefore leptin potentially affected the function of KCs. It has been presumed that leptin activated KCs and their phagocytic activity, and phagocytic activity of KCs and serum leptin concentrations were indeed decreased in MCDD rats in this study. In other words, because the amount of leptin secretion was low in MCDD rats, activation of KCs by leptin was attenuated and, thereby, the phagocytic activity of KCs was decreased. Although stimulation with leptin may be closely associated with the phagocytic activity of KCs, it is one of our experimental challenges to isolate and culture KCs from MCDD rats and determine whether addition of leptin will improve their phagocytic activity.

Although there is a report that contrast enhancement by contrast ultrasound was decreased in NASH patients compared to NAFLD and type C chronic hepatitis patients^[5], its pathogenesis has yet to be elucidated. By downregulating KCs and provoking leptin resistance, persistence of high concentrations of serum leptin levels decreases the activity of leptin and thereby reduces phagocytic activity in NASH patients. In this study, serum leptin concentrations were low and reduced leptin activity was one potential factor responsible for the pathogenesis. It should be possible to clinically diagnose NASH patients non-invasively, without liver biopsy, by quantifying contrast enhancement in contrast ultrasonography^[3]. Sensitivity and specificity for diagnosis of NASH differentiation from NAFLD are more than 90% and decrease in Levovist accumulation is the early stage of NASH.

In MCDD rats, pathological findings revealed fatty liver without inflammation or necrosis two weeks after the beginning of the MCDD, and the phagocytic activity of KCs was attenuated. These results suggest that it may be possible to diagnose NASH in human NASH patients at an early stage when inflammation, necrosis, and fibrosis specific for NASH have not developed. In addition, should early diagnosis of NASH be possible, early treatment would be feasible with prevention of progression to liver cirrhosis, and improvement of prognosis might be expected. It is necessary to accumulate clinical cases examined by a combination of contrast ultrasound and liver biopsy.

In conclusion, contrast enhancement in the late phase of contrast ultrasound was compared in MCDD rats and rats taking a regular chow. In the MCDD rats, accumulation of the contrast medium was attenuated compared to the control rats. As for the cause, a reduction in phagocytic activity by KCs was suspected, but activation by serum leptin might also be involved in the reduction of phagocytic activity.

COMMENTS

Background

Nonalcoholic steatohepatitis (NASH) is a disease that exhibits inflammation and fibrosis, and NASH may progress to liver cirrhosis and hepatocellular carcinoma. Early clinical diagnosis is important and difficult, and histological diagnosis based on liver biopsy is the only diagnostic method of NASH at the present time.

Research frontiers

Liver biopsy is somewhat invasive and may cause some complications, such as bleeding in the abdominal cavity or infection. Thus, a non-invasive method to diagnose NASH needs to be developed. It has been previously reported that liver-specific Kupffer images of contrast ultrasound can be used for differential diagnosis between NASH and nonalcoholic fatty liver disease (NAFLD).

Innovations and breakthroughs

The authors carried out a comparison of contrast ultrasonography between a NASH model and control rats. In the NASH model group, the intensity showed a significant decrease.

Applications

Contrast ultrasonography can be easily used to differentially diagnose NASH from NAFLD without liver biopsy.

Peer review

In the study, the authors demonstrated that phagocytic function of Kupffer cells from NASH liver is decreased. In this animal study, the authors also found that late phase contrast enhanced-ultrasound may be helpful in diagnosing NASH. Late phase contrast enhancement of NASH liver by ultrasound was lower compared to the simple fatty liver. The use of objective contrast quantification software appears promising. This might have implications in the diagnosis of NASH patients and in the evaluation of focal liver lesions in NASH patients; however further human studies are needed to evaluate this method.

REFERENCES

- 1 Ludwig J, Viggiano TR, McGill DB, Oh BJ. Nonalcoholic steatohepatitis: Mayo Clinic experiences with a hitherto unnamed disease. *Mayo Clin Proc* 1980; **55**: 434-438
- 2 Saadeh S, Younossi ZM, Remer EM, Gramlich T, Ong JP, Hurley M, Mullen KD, Cooper JN, Sheridan MJ. The utility of radiological imaging in nonalcoholic fatty liver disease. *Gastroenterology* 2002; **123**: 745-750
- 3 Iijima H, Moriyasu F, Tsuchiya K, Suzuki S, Yoshida M, Shimizu M, Sasaki S, Nishiguchi S, Maeyama S. Decrease in accumulation of ultrasound contrast microbubbles in non-alcoholic steatohepatitis. *Hepatol Res* 2007; **37**: 722-730
- 4 Watanabe R, Munemasa T, Matsumura M, Fujimaki M. Fluorescent liposomes for intravital staining of Kupffer cells to aid in vivo microscopy in rats. *Methods Find Exp Clin Pharmacol* 2007; **29**: 321-327
- 5 Moriyasu F, Iijima H, Tsuchiya K, Miyata Y, Furusaka A, Miyahara T. Diagnosis of NASH using delayed parenchymal imaging of contrast ultrasound. *Hepatol Res* 2005; **33**: 97-99
- 6 Kirsch R, Clarkson V, Shephard EG, Marais DA, Jaffer MA, Woodburne VE, Kirsch RE, Hall Pde L. Rodent nutritional model of non-alcoholic steatohepatitis: species, strain and sex difference studies. *J Gastroenterol Hepatol* 2003; **18**: 1272-1282
- 7 Koppe SW, Sahai A, Malladi P, Whittington PF, Green RM. Pentoxifylline attenuates steatohepatitis induced by the methionine choline deficient diet. *J Hepatol* 2004; **41**: 592-598
- 8 Romestaing C, Piquet MA, Bedu E, Rouleau V, Dautresme M, Hourmand-Ollivier I, Filippi C, Duchamp C, Sibille B. Long term highly saturated fat diet does not induce NASH in Wistar rats. *Nutr Metab (Lond)* 2007; **4**: 4
- 9 Adams LA, Lymp JF, St Sauver J, Sanderson SO, Lindor KD, Feldstein A, Angulo P. The natural history of nonalcoholic fatty liver disease: a population-based cohort study. *Gastroenterology* 2005; **129**: 113-121
- 10 Palekar NA, Naus R, Larson SP, Ward J, Harrison SA. Clinical model for distinguishing nonalcoholic steatohepatitis from simple steatosis in patients with nonalcoholic fatty liver disease. *Liver Int* 2006; **26**: 151-156
- 11 George J, Pera N, Phung N, Leclercq I, Yun Hou J, Farrell G. Lipid peroxidation, stellate cell activation and hepatic fibrogenesis in a rat model of chronic steatohepatitis. *J Hepatol* 2003; **39**: 756-764
- 12 Sahai A, Malladi P, Pan X, Paul R, Melin-Aldana H, Green RM, Whittington PF. Obese and diabetic db/db mice develop marked liver fibrosis in a model of nonalcoholic steatohepa-

- titis: role of short-form leptin receptors and osteopontin. *Am J Physiol Gastrointest Liver Physiol* 2004; **287**: G1035-G1043
- 13 **Yanagisawa K**, Moriyasu F, Miyahara T, Yuki M, Iijima H. Phagocytosis of ultrasound contrast agent microbubbles by Kupffer cells. *Ultrasound Med Biol* 2007; **33**: 318-325
- 14 **Iijima H**, Sasaki S, Moriyasu F, Suzuki S, Yoshida M, Horibe T, Tsuchiya K. Dynamic US contrast study of the liver: Vascular and delayed parenchymal phase. *Hepatol Res* 2007; **37**: 27-34
- 15 **Watanabe R**, Matsumura M, Chen CJ, Kaneda Y, Fujimaki M. Characterization of tumor imaging with microbubble-based ultrasound contrast agent, sonazoid, in rabbit liver. *Biol Pharm Bull* 2005; **28**: 972-977
- 16 **Suzuki S**, Iijima H, Moriyasu F, Sasaki S, Yanagisawa K, Miyahara T, Oguma K, Yoshida M, Horibe T, Ito N, Kakizaki D, Abe K, Tsuchiya K. Differential diagnosis of hepatic nodules using delayed parenchymal phase imaging of levovist contrast ultrasound: comparative study with SPIO-MRI. *Hepatol Res* 2004; **29**: 122-126
- 17 **Toft KG**, Hustvedt SO, Hals PA, Oulie I, Uran S, Landmark K, Normann PT, Skotland T. Disposition of perfluorobutane in rats after intravenous injection of Sonazoid. *Ultrasound Med Biol* 2006; **32**: 107-114
- 18 **Diehl AM**. Nonalcoholic steatosis and steatohepatitis IV. Nonalcoholic fatty liver disease abnormalities in macrophage function and cytokines. *Am J Physiol Gastrointest Liver Physiol* 2002; **282**: G1-G5
- 19 **Diehl AM**. Lessons from animal models of NASH. *Hepatol Res* 2005; **33**: 138-144
- 20 **Lin HZ**, Yang SQ, Chuckaree C, Kuhajda F, Ronnet G, Diehl AM. Metformin reverses fatty liver disease in obese, leptin-deficient mice. *Nat Med* 2000; **6**: 998-1003
- 21 **Loffreda S**, Yang SQ, Lin HZ, Karp CL, Brengman ML, Wang DJ, Klein AS, Bulkley GB, Bao C, Noble PW, Lane MD, Diehl AM. Leptin regulates proinflammatory immune responses. *FASEB J* 1998; **12**: 57-65
- 22 **Sakaida I**, Jinhua S, Uchida K, Terai S, Okita K. Leptin receptor-deficient Zucker (fa/fa) rat retards the development of pig serum-induced liver fibrosis with Kupffer cell dysfunction. *Life Sci* 2003; **73**: 2491-2501

S- Editor Tian L L- Editor Logan S E- Editor Xiong L